The Role of Drug–Drug Interactions in Hydrogel Delivery Systems: Experimental and Model Study

Filippo Rossi[+],*[a] Franca Castiglione[+],[a] Monica Ferro,[a] Marta Moioli,[a] Andrea Mele,[a, b] and Maurizio Masi[a]

To address the increasing need for improved tissue substitutes, tissue engineering seeks to create synthetic, three-dimensional scaffolds made from polymeric materials able to incorporate cells and drugs. The interpretation of transport phenomena is a key step, but comprehensive theoretical data is still missing and many issues related to these systems are still unsolved. In particular, the contribution of solute–solute interactions is not yet completely understood. Here, we investigate a promising agar–carbomer (AC) hydrogel loaded with sodium fluorescein (SF), a commonly used drug mimetic. The self-diffusion coefficient of SF in AC formulations was measured by using high resolution magic angle spinning NMR spectroscopy (HR-MAS NMR). Starting from experimental data, a complete overview on SF transport properties is provided, in particular a mathematical model that describes and rationalizes the differences between gel and water environments is developed and presented. The hydrogel molecular environment is able to prevent SF aggregation, owing to the adsorption mechanism that reduces the number of monomers available for oligomer formation at low solute concentration. Then, when all adsorption sites are saturated free SF molecules are able to aggregate and form oligomers. The model predictions satisfactorily match with experimental data obtained in water and the gel environment, thus indicating that the model presented here, despite its simplicity, is able to describe the key phenomena governing device behavior and could be used to rationalize experimental activity.

1. Introduction

Hydrogels are three-dimensional polymeric networks, which are insoluble in aqueous environments, due to physical and/or chemical crosslinks, and able to retain large amounts of water or biological fluids.[1,2] In the last couple of decades, hydrogels have shown great promise for many biological and biomedical applications, and significant progress has been made in designing, synthesizing, and using these materials. Recent developments include the design and synthesis of novel hydrogels and their use in tissue engineering, drug delivery, and bionanotechnology.[3–5] In addition, other applications, such as analytical separation methods with a diffusion gradient in a thin film or gel electrophoresis, involve hydrogel systems.[6,7] Hence, to improve performance of materials in these fields, a deep understanding of solute transport in gel matrices is highly important.[8–11] Indeed, effective solute transport is one of the most critical design parameters for hydrogels in these systems.[9,10,12,13] Mass-transport parameters determine how nutrients, gasses, waste products, and bioactive agents, such as growth factors and drugs, are exchanged within scaffolds or are delivered by the gel. Convection usually does not play a significant role in the movement of solutes through hydrogel matrices, except in hydrogels with large micropores or forced flow conditions. Diffusion alone is commonly regarded as the driving transport phenomenon.[14–16] Despite the high simplicity, in terms of mass transport for chemical engineering applications, several problems arise; available studies often show low or even no accordance to descriptive theories and, more generally, this topic is still much debated.[17,18] Several works on drug-delivery systems are centered on pure Fickian diffusion with degradation and swelling contributions.[19,20] However, especially at low drug concentrations, several other mechanisms, such as drug–polymer interactions, that could influence mass transport take place and cannot be neglected for an optimal device design.[11] In this work, we studied the release of sodium fluorescein (SF), a commonly used drug-mimetic molecule,[21–23] chosen for its steric hindrance and its resemblance to many corticosteroids and anti-inflammatory drugs (for example, methylprednisolone, ibuprofen, and estradiol) used in pharmacotherapy.[24,25] Moreover, SF molecules present a common tendency of anti-inflammatory drugs: aggregation in dimers and trimers.[26,27] The main aim of this work is to investigate the role of drug–drug interactions within an hydrogel delivery system and to then compare the results with the ones collected in an aqueous environment. The chosen hydrogel, specifically developed for central-nervous-system repair strategies, was obtained by synthesis from statistical block polycon-

[a] *Dr. F. Rossi,[+] Dr. F. Castiglione,[+] M. Ferro, M. Moioli, Prof. Dr. A. Mele, Prof. Dr. M. Masi*
Department of Chemistry, Materials and Chemical Engineering "Giulio Natta", Politecnico di Milano, via Mancinelli 7, 20131 Milan (Italy)
E-mail: filippo.rossi@polimi.it

[b] *Prof. Dr. A. Mele*
CNR-ICRM, via Luigi Mancinelli 7, 20131 Milan (Italy)

[+] *These authors equally contributed to this work.*

densation between agarose and carbomer 974P (briefly termed as AC, acronymic of their main components), together with crosslinkers. SF self-diffusion coefficients were measured in water and in gel by means of pulsed magnetic field gradients spin-echo (PGSE) nuclear magnetic resonance (NMR) spectroscopy using the high-resolution magic angle spinning (HR-MAS) technique.[28–30] Then, to understand the differences in terms of drug transport through water solution and hydrogel environment, we propose a mathematical model based on adsorption mechanisms firstly applied by Carta and Schirmer on polysaccharide-based hydrogels for chromatography[31] and then optimized by our research group for hydrogel-based drug-delivery systems.[32] In addition, we considered the aggregation contribution, which takes place in a different manner between the two environments and is common in several commonly-used drugs.[33,34] This approach represents the possibility to predict release behavior, and therefore, to improve medical prospects.

Experimental Section

Materials

Carbomer 974P (CAS 151687-96-6) with high molecular weight (about 1 MDa), was provided by Fagron (The Netherlands), triethylamine (TEA; CAS 121-44-8) with high purity was purchased from Sigma–Aldrich (Germany). The solvent used was phosphate buffer saline solution (PBS), purchased from Sigma–Aldrich (Germany). For NMR and HR-MAS analysis deuterated PBS was used to avoid overlapping of the ^{1}H signal of SF with those of PBS. The other polymer involved in the reaction is agarose (CAS 9012-36-6), purchased from Invitrogen (USA) and having a molecular weight of about 300 kDa. Lastly, sodium fluorescein (SF, CAS 2321-07-5) was provided by Sigma–Aldrich (Germany). All materials were used as received.

Hydrogel Synthesis and Drug Loading

The synthesis and drug loading were performed in accordance with previous works.[32,35] Briefly, Carbomer 974P (0.5 g) was stirred and neutralized to pH 7.4 in deuterated PBS solution. Agarose powder (0.5% w/v) was subsequently added and the system was electromagnetically heated up to 80 °C to induce the condensation reactions. Then, SF was added to the polymeric formulation as an aqueous solution, before the cross-linking procedure and thus sol/gel transition occurs. SF was loaded in a range from 5 to 200 mg mL^{-1}, to clearly explore concentration effects on transport properties. The gelling solution was then placed in steel cylinders (0.5 mL each and with the same dimensions of a standard well in a 48 plate) and left to rest at 37 °C until reaching complete gelation and thermal equilibrium. The formation of ester bonds between agarose and carbomer, which leads to the setting up of hydrogel networks, was described in previous works, where we discussed the chemical nature of agarose–carbomer based hydrogels.[21,36] Owing to these reactions, AC hydrogels are anionic and this electrostatic nature was confirmed by FTIR and mass equilibrium swelling at different pH. The acronyms for the hydrogels are harmonized with previous studies.[32] The crosslinking process during hydrogel synthesis produces a distribution of polymer-chain molecular weights between junctions and, correspondingly, a distribution of mesh sizes, as observed in previous works. The three-dimensional structure of a gel could be described as polymer chains interconnected forming meshes filled with aqueous solution. Mesh size (ξ) describes the average distance between crosslinks in a polymer network and can be estimated with Flory–Rehner theory.[37,38] The complete and exhaustive treatment of Flory–Rehner theory applied to AC hydrogels was studied and presented in previous works:[32] ξ 45 nm, average molecular weight between two following cross links (M_c) 2500 g mol^{-1}, cross-linking density (ν_e) 28 kmol cm^{-3}, and porosity (ε) 0.9.

HR-MAS NMR spectroscopy

HR-MAS NMR spectra were recorded in accordance with previous works.[21,30,32] In brief, the ^{1}H NMR spectra of the hydrogel systems were recorded on a Bruker Avance spectrometer operating at 500 MHz proton frequency, equipped with a dual $^{1}H/^{13}C$ HR-MAS probe head for semisolid samples. Self-diffusion coefficients were measured by diffusion ordered correlation spectroscopy (DOSY) experiments, based on a pulsed field gradient spin-echo (PGSE) approach. A pulsed gradient unit capable of producing magnetic field pulse gradients in the z direction up to 53 G cm^{-1} was used. These experiments were performed using the bipolar pulse longitudinal eddy current delay (BPPLED) pulse sequence. In the z direction, the duration of the magnetic field pulse gradients (δ) and the diffusion times (Δ) were optimized for each sample to obtain complete dephasing of the signals with the maximum gradient strength. In each DOSY experiment, a series of 64 spectra with 32k points were collected. For each experiment 32 scans were acquired. For the investigated samples, Δ was set to 0.1 s, whereas the δ values were in the range 0.7–2 ms. The pulse gradients were increased incrementally from 2 to 95% of the maximum gradient strength in a linear ramp. The temperature was set and controlled at 37 °C with an air flow of 535 l h^{-1} to avoid any temperature fluctuations due to sample heating during the magnetic field pulse gradients.

Adsorption Kinetics

Adsorption isotherms and batch uptake rates, obtained by material balance and drug concentration profiles in the gels were determined following literature methods.[31] Briefly, the adsorption isotherms were obtained by suspending small gel samples in SF solutions with different initial concentrations and mixing for 8 h. Based on the kinetic measurements, this time was estimated to be sufficient to reach equilibrium even with the slowest resin considered. For the batch uptake rates, the agarose particles were suspended in a protein solution in an agitated vessel and the amount adsorbed was obtained from the residual drug concentration at each time.

Mathematical Model

The model discussed later on was developed with MatLab© suite, using the *lsqcurvefit* function to match experimental data with the proposed physical chemical description.

Statistical analysis

Where applicable, experimental data were analyzed using analysis of variance (ANOVA). Statistical significance was set to p value $<$ 0.05. Results are presented as mean value $\pm$ standard deviation. Spectroscopic data presents a standard deviation of about 5%, due to intrinsic instrumental precision.

2. Results and Discussion

2.1. HR-MAS NMR Spectroscopy: Chemical Shift and Self-Diffusion Coefficients of SF

The issue of SF self-aggregation in aqueous solutions has already been addressed in previous work.[30] For the sake of clarity, we summarize the main concepts here. The self-aggregation of SF in D_2O solutions was assessed by the inspection of linewidths in the ^1H NMR spectra. High resolution NMR bands were detectable up to a SF concentration of 100 mg mL^{-1}, showing the threshold for the formation of aggregates. Theoretical calculations demonstrated that SF dimers have a minimum-energy symmetric structure that is stabilized by π–π interactions, even at low concentrations.[22] At higher concentrations, more-complex aggregates were found. This effect was more prominent for the protons H_3, H_4, H_7, and H_8, due to intermolecular H bonds and π–π stacking upon dimer formation.

The ^1H NMR spectrum of SF in AC hydrogels is characterized by broad signals, due to residual solid-state effects related to dipole-dipole coupling. This shortcoming makes the NMR spectra acquired by conventional liquid-state probe heads completely useless for the structural and dynamical characterization of the materials. Here, the use of the HR-MAS technique allowed well-defined spectra of SF-loaded hydrogels to be obtained.[21,32] The HR-MAS spectral signals are not affected by hydrogel matrix interference, with well-resolved peaks for the investigated molecule. HR-MAS NMR spectroscopy opened up the possibility of using the whole repertoire of high resolution NMR pulse sequences to investigate semisolid materials, including heterogeneous systems, ex vivo medical specimens, and soft matter. The HR-MAS NMR spectra of the examined systems (Figure 1) do not show the marked concentration-dependent line broadening detected in D_2O, and the spectral lines remained well-resolved even at high SF concentrations.

The large variations in chemical shift with increasing SF concentration selectively experienced by H_2, H_3, and H_4 can be accounted for by considering the shielding effects, due to the aromatic-ring current in dimer formation. However, the formation of significantly larger aggregates seems to be unrealistic in this concentration range, as proven by the small signal broadening for all the spectral peaks. Therefore, the molecular state of SF in AC gels in the explored concentration range can be reasonably described as ranging from single solvated molecules to small aggregates, such as dimers or trimers.[22] Scheme 1 illustrates a schematic representation of the two systems: water with a higher formation of oligomers and a gel environment with less SF aggregation.

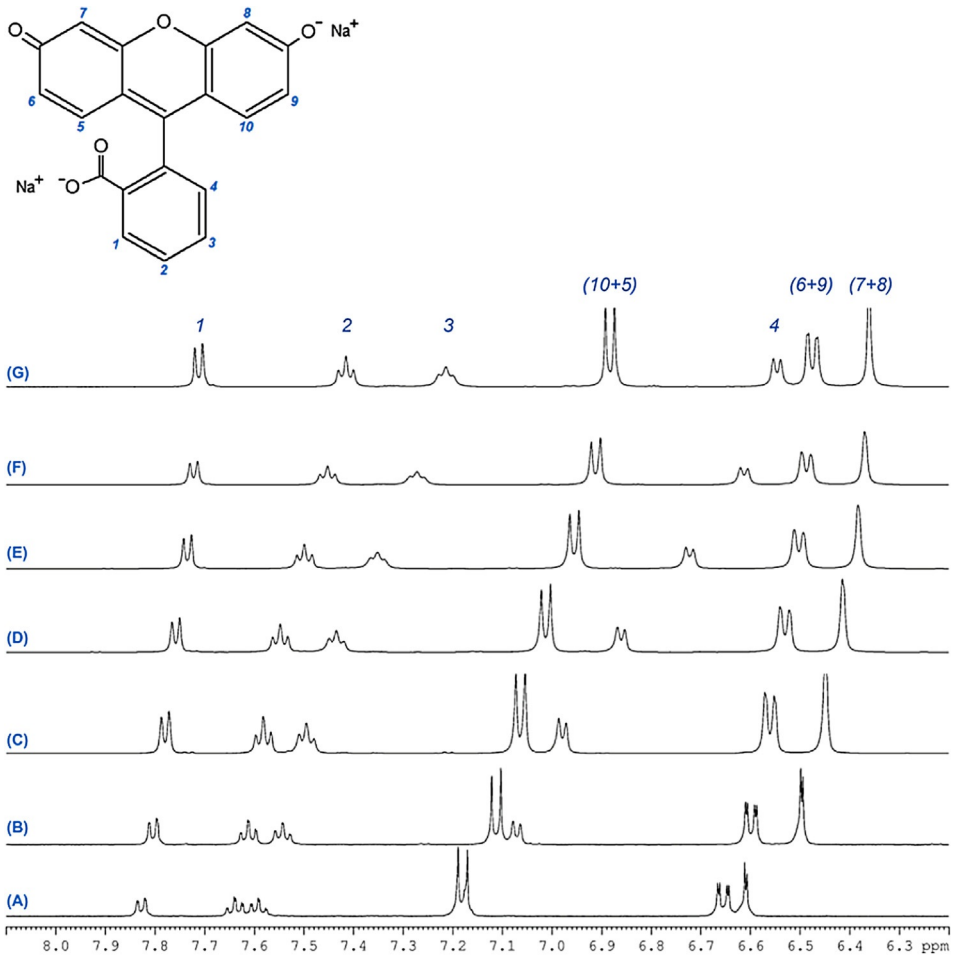

Figure 1. ^1H HR-MAS spectra of SF in gel AC1 at several concentrations: A) 6, B) 12.5, C) 25, D) 50, E) 100, F) 150, and G) 200 mg mL^{-1}. The top left inset shows the molecular structure and atom numbering of SF.

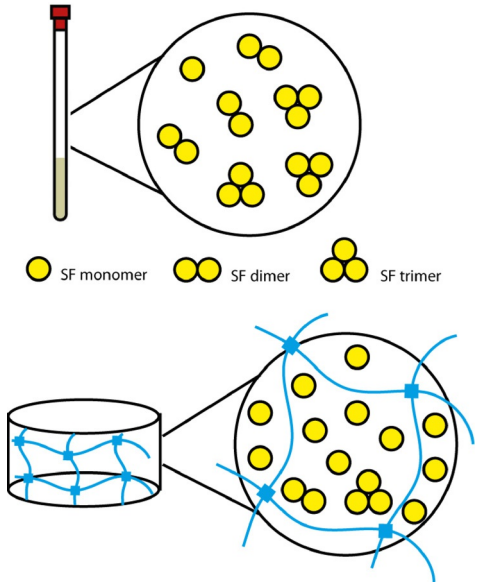

Scheme 1. Pictorial representation of the different SF aggregation in liquid and semi-solid (gel) environments.

The experimental determination of the self-diffusion coefficients for SF at different concentrations was carried out by PGSE-NMR experiments. These values are reported in Table 1, together with the SF diffusion values in water solutions. SF diffusivity was measured at different concentrations both in gel and in water, by HR-MAS NMR and liquid-state NMR spectroscopy, respectively, to study and understand the differences related to the environment of diffusion. As shown in Table 1, the diffusion coefficient of SF in D_2O decreases from 4.5×10^{-10} to 2.9×10^{-10} $m^2 s^{-1}$, thus indicating aggregation into larger molecular associations in concentrated solutions.

Table 1. Diffusion coefficients of SF at different concentrations in: water solution (D_{water}), in AC hydrogel (D_{gel}) and their ratios with respect to SF diffusivity at infinite dilution (D_{gel}/D_{inf} and D_{water}/D_{inf}).

SF concentration [mg mL^{-1}]	D_{gel}[a] [m^2 s^{-1}]	D_{water}[a] [m^2 s^{-1}]	D_{gel}/D_{inf}	D_{water}/D_{inf}
10	5.4 ± 0.5	4.5 ± 0.4	0.98 ± 0.06	0.82 ± 0.08
50	4.7 ± 0.4	2.9 ± 0.3	0.85 ± 0.07	0.53 ± 0.06
100	4.2 ± 0.5	2.9 ± 0.3	0.76 ± 0.05	0.53 ± 0.05
150	3.3 ± 0.3	2.4 ± 0.3	0.61 ± 0.06	0.44 ± 0.05
200	3.9 ± 0.4	2.9 ± 0.3	0.70 ± 0.07	0.53 ± 0.05

[a] All values have to be multiplied by 10^{-10}.

It is also evident from Table 1 that SF diffusivity in the gel decreases, as SF concentration increases from 5.4×10^{-10} to 3.9×10^{-10} $m^2 s^{-1}$. However the most important and counter-intuitive result is that, at every SF concentration, diffusivity in the gel is higher than in water. As mentioned, this behavior seems to be unrealistic, because, following the Stoke–Einstein equation, diffusivity is inversely proportional to diffusant viscosity. It is indeed well-known that, in colloids, diffusivity is the ratio between thermal forces typical of Brownian motion and viscous forces applied by the system (here the water solution and gel) to the diffusing agent (here SF). In this case, the viscosity of water is lower than that of the gel and the logical consequence would be higher diffusivity values in water rather than in the gel system. To justify this mismatch, it is obvious that other mechanisms should be considered and taken into account. In Table 1, we also present diffusivity at certain concentrations divided by diffusivity at infinite dilution both in the gel and in water.

3.2. Modeling SF Diffusion Coefficients in Water

In the concentration range from 1.8×10^{-3} to 250 mg mL^{-1} the fluorescein dianion associates forming both dimers and trimers.[39] The equilibrium constants for the dimerization and trimerization are [Eqs. (1) and (2)]:

$$M + M \rightarrow D \quad K_d = 5.0 \tag{1}$$

$$M + D \rightarrow T \quad K_t = 10.0 \tag{2}$$

Where M represents a monomer, D is a dimer, T is a triplet, K_d is the equilibrium constant for SF dimerization, and K_t is the equilibrium constant for SF trimerization.

A hydrogen bond is responsible for dimer formation, although contributions from van der Waals forces are possible, especially in the case of trimer formation. Following this direction we could calculate diffusivity as [Eq. (3)]:

$$D_{water} = \frac{C_M}{C_{tot}} \cdot D_M + \frac{C_D}{C_{tot}} \cdot D_D + \frac{C_T}{C_{tot}} \cdot D_T \tag{3}$$

where C_M is monomer concentration, C_D is dimer concentration, C_T is trimer concentration, and C_{tot} the total SF present, D_M is monomer diffusivity, D_D is dimer diffusivity, D_T is trimer diffusivity from a study by Casalini et al.[22] In Figure 2, mathematical modeling results are presented together with experimental data. In particular ,the three lines are related to three different assumptions: 1) only monomers are present, $C_{tot} = C_M$ (red); 2) monomers and dimers are present, $C_{tot} = C_M + 2C_D$

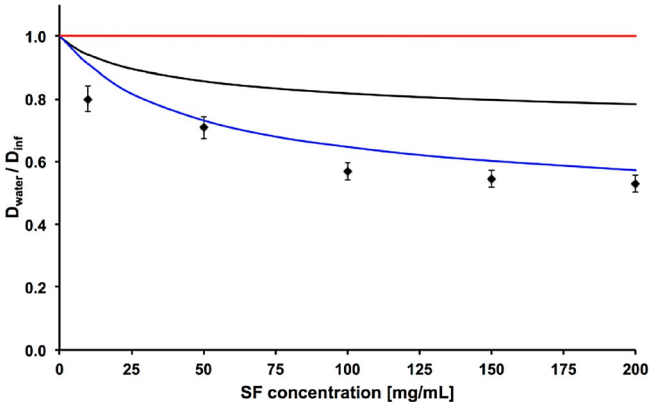

Figure 2. Diffusion normalized coefficients (D_{water}/D_{inf}), experimental data (dots), and model trend (lines): a) red, only monomers; b) black, monomers and dimers; and c) blue, monomers, dimers and trimers.

(black); and 3) monomers, dimers, and trimers are present, $C_{tot} = C_M + 2C_D + 3C_T$ (blue). It is evident that the introduction of the terms related to dimers and trimers are fundamental to understand the phenomena involved and match the experimental data. In addition, SF aggregation increases as SF concentration increases with a consequent reduction in the diffusivity value.

3.3. Modeling SF Diffusion Coefficients in Gel

As shown in previous work,[21] the application of the Fick model to drug-release experiments provides reliable diffusion coefficients for low concentrations of SF, but cannot be used to study the effect of concentration on mass transport. It is well-known that, in the absence of a drug-concentration gradient (as in the present case), the drug-release rate is not expected to be influenced by the drug concentration.[40] On the contrary, drug motion within the pores of the polymeric matrix is highly influenced by the environment and by the other drug molecules.

This mismatch cannot be addressed by using the Fick equation, and other types of mechanisms should be postulated. In particular, here we propose a model that is able to describe the experimental behavior. The model is based on the following hypotheses: 1) The drug can be adsorbed onto the three-dimensional polymeric network only if it is in the monomeric state. The adsorption step thus reduces the contribution of any drug-aggregation phenomena. As a consequence, at low concentration of SF the most important phenomenon is adsorption within hydrogel pores, which reduces the amount of SF available for the formation of dimers and trimmers. 2) As the amount of SF is increased, the adsorption sites are progressively saturated and then SF can diffuse more quickly, as in water, and diffusion is driven only by the concentration gradient. The rationale for this is based on the observation that the ratio between the mean gel-network mesh size and the mean SF hydrodynamic radius is extremely low—diffusant molecules are mobile inside the entangled hydrogel network, and thus, diffuse with a high free motion. The adsorption mechanism is thus expected to play a dominant role at low SF concentrations, whereas its role is negligible for higher drug concentrations. Previous works by Kim and co-workers on in vivo applications of methylprednisolone released from hydrogels[24] revealed the therapeutic efficacy for a concentration of 10 mg mL^{-1} (200 μg each animal). As reported, at low drug concentrations, where steroids show high efficacy, the adsorption phenomenon should be considered when describing the drug-transport mechanisms. A pictorial representation of the model is shown in Figure 4, where the solid lines represent the negatively charged AC matrix, the white circles represent the SF molecules adsorbed onto the network backbone, the yellow circles represent SF molecules that are free to move within the network. SF molecules may either undergo adsorption or diffusion. The latter points are shown in Figure 3: the green arrows indicate diffusion of SF monomers within the polymeric network, whereas the red arrows show the subsequent adsorption onto the polymer matrix. If all adsorption sites are saturated, SF monomers continue to diffuse, thus they are likely to collide with other SF monomers (black arrow) and can form dimers and trimers.

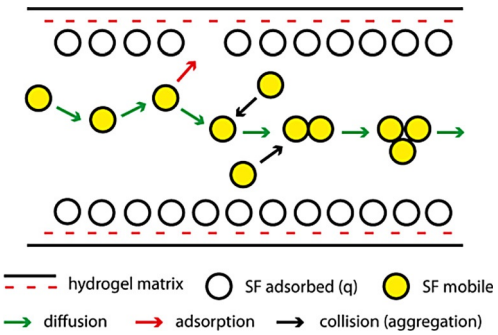

Figure 3. Pictorial representation of the partitioning model.

The experimental diffusion constants detected are the rapid-exchanged values resulting from the weighted average of both the adsorbed and free diffusion rates.

At this stage, we propose a mathematical model accounting for the steps described above. The adsorbed SF concentration is given by q, as determined from the adsorption Langmuir isotherm (Figure 4).[31] The isotherm is highly favorable at low drug concentrations. Thus, the Langmuir isotherm (K) was used to fit the data according to Equation (4):

$$q = \frac{q^{\infty} \cdot K \cdot C_G}{1 + K \cdot C_G} \quad (4)$$

where q^{∞} is the maximum total adsorbed concentration of SF and C_G is the SF concentration within the hydrogel. A fitted line is presented in Figure 5 and calculated parameters are: $q^{\infty} = 32$ mg cm^{-3} and $K = 1370$ cm^3 mg^{-1}.

The equation accounting for the aggregation with adsorption could be written as follows, assuming that, in a hydrogel network, the SF molecules can be grouped into four categories: monomers, dimers, trimers and adsorbed molecules [Eq. (5)]:

$$C_{tot} = C_M + 2 \cdot C_D + 3 \cdot C_T + \frac{1-\varepsilon}{\varepsilon} \cdot \frac{q^{\infty} \cdot K \cdot C_M}{1 + K \cdot C_M} \quad (5)$$

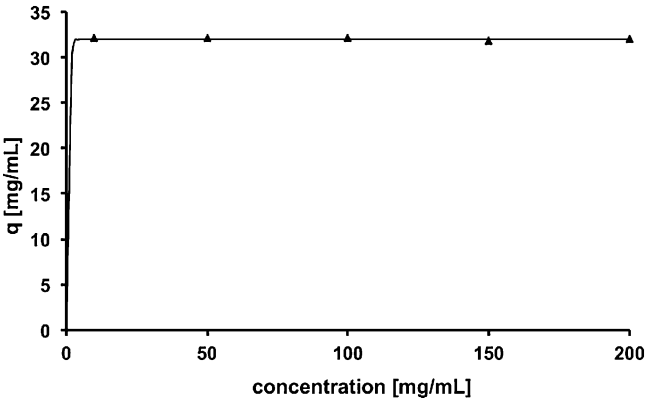

Figure 4. Adsorption isotherm for SF on an AC hydrogel. The line is based on Equation (2).

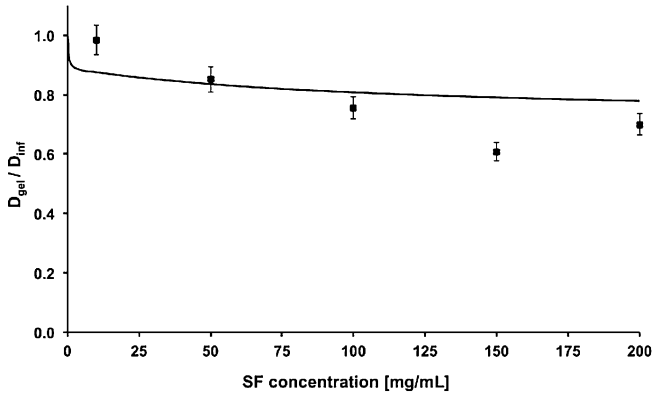

Figure 5. Diffusion normalized coefficients (D_{gel}/D_{inf}), experimental data (dots) and model trend (lines).

The joint contribution of diffusion and adsorption can be described by Equation (6):

$$\varepsilon \cdot \frac{\partial C_G}{\partial t} = \varepsilon \cdot D_{gel} \cdot \frac{\partial^2 C_G}{\partial x^2} - (1-\varepsilon) \cdot \frac{\partial q}{\partial t} \quad (6)$$

where ε is the gel porosity calculated in previous works[21] and C_G is SF concentration within the hydrogel. From Equation (6) we can easily obtain the D_{gel} ratio [Eq. (7)]:

$$D_{gel} = \frac{\varepsilon}{\varepsilon + (1-\varepsilon) \cdot \frac{q^{\infty} \cdot K}{(1+K \cdot C_G)^2}} \cdot \left(\frac{C_M}{C_{tot}} \cdot D_M + \frac{C_D}{C_{tot}} \cdot D_D + \frac{C_T}{C_{tot}} \cdot D_T \right) \quad (7)$$

The model was tested against the experimental values presented in Table 1. The experimental and calculated data are presented in Figure 5.

The good agreement between the model (line) and experiments (■) underlines that the adsorption isotherm together with diffusion through pores and aggregation can describe the mechanisms involved in SF release from a 3D polymeric network. In particular: 1) The drug is first partitioned and adsorbed into the hydrogel pores. The amount of adsorbed drug is given by q^{∞}, as determined from the adsorption isotherm. 2) At higher drug concentrations, the monomers diffusing within the polymeric network can collide with other monomers and then aggregate to dimers and trimers.

3.4. Oligomer Concentrations in Water and in Gel

As described before, the mismatch between the Stoke–Einstein equation and experimental diffusivity obtained with the HR-MAS technique, could be explained by different amounts of oligomers in the gel compared with the water solution. In particular, the adsorption mechanism, which is especially active at low drug concentrations, decreases the amount of the available monomers. In Figure 6 A, the curves related to monomers in water and the gel are presented; the lower amount of monomers at low drug concentrations in the gel reveals that the adsorption process decreases the amount of SF capable to diffuse through the system.

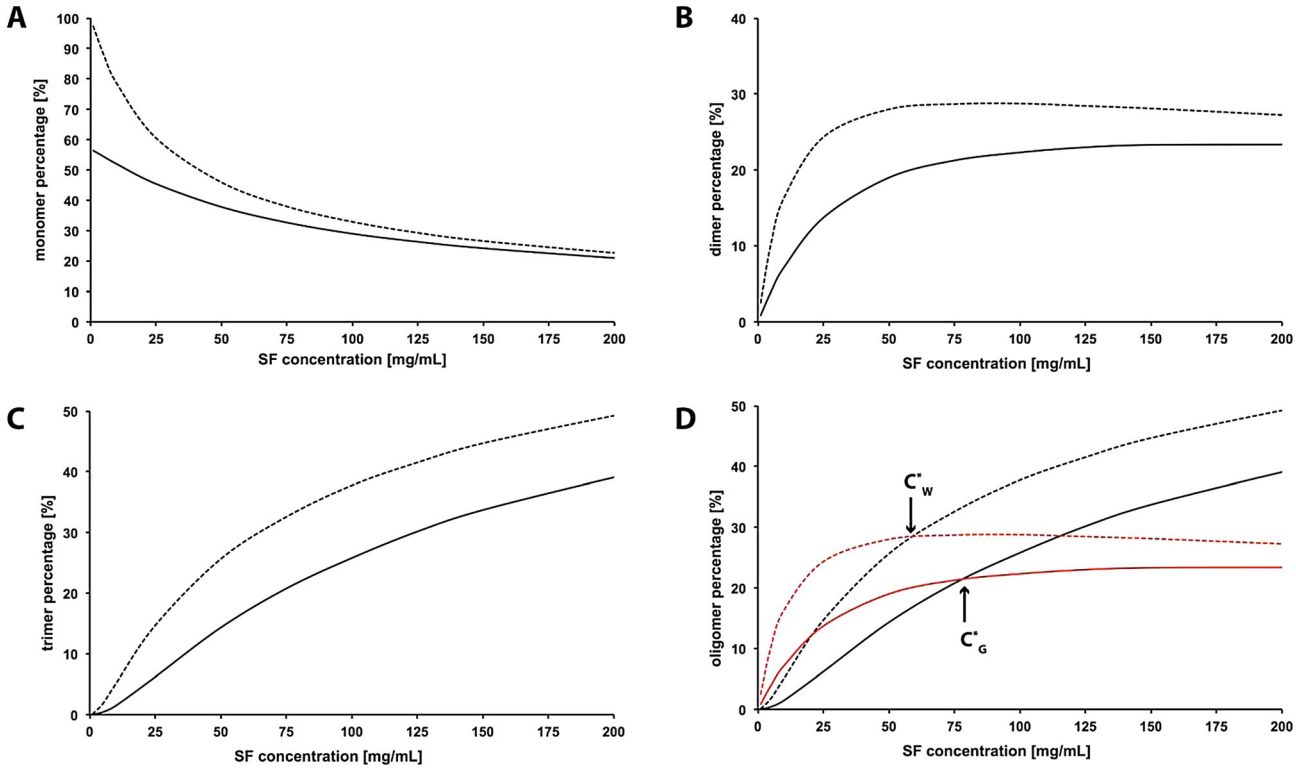

Figure 6. Oligomer percentage in water (dashed line) and in gel (line): A) monomers, B) dimers, and C) trimers. D) Critical concentrations for water (C_W*) and gel (C_G*).

Moreover, higher SF concentrations tends to offset the difference between the gel and water, because all of the adsorption sites are saturated and the residual solute is free to move and aggregate to dimers and trimers. Trends related to dimers and trimers in the gel (line) and in water (dashed line) are presented in Figures 6B and C. In accordance with Figure 6A, the amount of dimers and trimers in the gel is lower than in water, underlining the fact that hydrogel systems can hamper their formation. In addition, the difference between the two lines decreases with increasing SF concentration, due to saturation of adsorption sites. Moreover at high concentrations, trimers are favored and, considering the intersection between the dimer and trimer curves (Figure 6D) in water and in the gel, it is visible that in the first case (critical SF concentration in water; C_W*) for SF concentration higher than 50 mg mL^{-1}, trimers are more abundant than dimers. Under gel conditions, this critical concentration (C_G*) is higher, around 75 mg mL^{-1}; this is easily explained by considering that the limiting aggregation step is the collision between monomers, of which there are fewer in gel network.

3.5. Role of Porosity

Starting from Figure 6, we investigated other scenarios to understand the aggregation mechanism with the aim of controlling and tuning the release rates of SF. In Figure 7, the oligomer (monomers, dimers and trimers) trends are presented for different hydrogel porosity values.

The adsorption kinetics becomes slower as gel porosity decreases, and consequently, the adsorption contribution; for these reasons, the amounts of monomers, dimers and trimers available decrease as porosity increases. In Figure 7D, the critical concentrations (C_G*) defined above are presented for different porosity values. As expected this value is not dependent on ε, because the adsorption mechanism happens mainly at low SF concentration and does not influence aggregation itself. Indeed its role is only related to the reduction of the amount of monomers available.

Tuning hydrogel porosity seems to be a promising method to control solute aggregation, and consequently, mass transport through network pores. In Figure 8 is presented the dependence of diffusivity in gel on hydrogel porosity; upon decreasing gel porosity, it is evident that the adsorption kinetics is slower. In particular, at SF concentrations at which the adsorption mechanism is not negligible, the concentration increases with decreasing porosity.

4. Conclusions

The development of multicomponent material systems, that is, systems integrating multiple materials with diverse physicochemical properties, is one of the hot topics in the field of controlled drug delivery. The release kinetics is, thus, driven by multiple factors and cannot be described by a single mathematical model that considers only pure Fickian diffusion and swelling/degradation contributions. To better elucidate drug-transport mechanisms and predict transport behavior, it is cru-

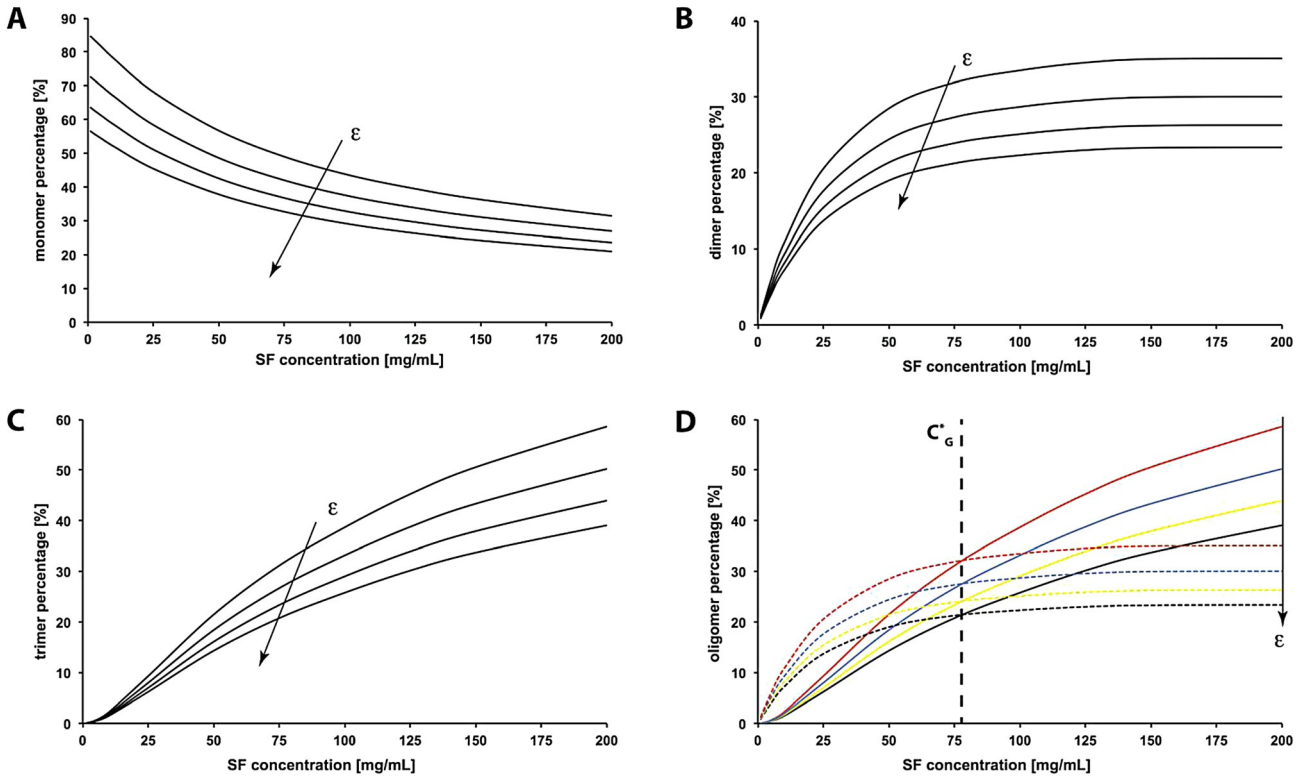

Figure 7. Oligomers percentage in gel as function of porosity (ε): A) monomers, B) dimers, and C) trimers. D) Critical concentrations for gel (C_G*) depending on network porosity; lines of the same color present the same porosity.

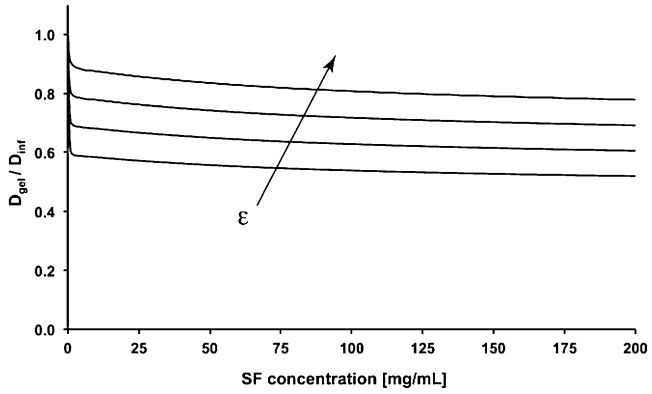

Figure 8. Simulations of SF normalized diffusivity (D_{gel}/D_{inf}) tuning hydrogel porosity.

cial to establish the connection between measurements at the molecular level and drug-release kinetics. In the present work, solute diffusivity was measured by means of the HR-MAS NMR spectroscopy, giving a counterintuitive result, drug diffusivity in water appears to be lower compared with that in the gel network, which was investigated. In this scenario, the present work provides a deeper insight of solute–solute interactions during their transport within polymeric matrices depending on the environment: gel state or liquid solution. This model successfully predicts the experimental trends; the aggregation phenomena in the gel are inhibited compared with those in water, where dimers and trimers are most abundant. The rationale lies in the solute adsorption, as the key mechanism, taking place and reducing the amount of monomers available for aggregation. This phenomenon is more important at low drug concentrations, where adsorption contribution seems to be higher and could not be neglected with a consequent lower amount of monomers present in the gel than in water. Upon increasing drug concentration, to saturate all adsorption sites, free monomers in the network are subjected to aggregation to dimers and trimers. Solute–solute interactions are also highly dependent on hydrogel porosity; the higher the porosity, the lower the amount of monomers that can aggregate with a consequent higher diffusivity. From an applications point of view, it is thus possible to optimize the experimental activity, which can be expensive and time-consuming, through a "model driven" experimental approach, thus avoiding the classic "trial and error" modus operandi; a more careful management of resources is nowadays an implicit need to be fulfilled in all research and development activities.

Keywords: adsorption · diffusion · drug delivery · gels · NMR spectroscopy

[1] B. V. Slaughter, S. S. Khurshid, O. Z. Fisher, A. Khademhosseini, N. A. Peppas, *Adv. Mater.* **2009**, *21*, 3307 – 3329.
[2] N. Annabi, A. Tamayol, J. A. Uquillas, M. Akbari, L. E. Bertassoni, C. Cha, G. Camci-Unal, M. R. Dokmeci, N. A. Peppas, A. Khademhosseini, *Adv. Mater.* **2014**, *26*, 85 – 124.
[3] R. Langer, *Adv. Mater.* **2009**, *21*, 3235 – 3236.
[4] F. Rossi, G. Perale, S. Papa, G. Forloni, P. Veglianese, *Expert Opin. Drug Delivery* **2013**, *10*, 385 – 396.
[5] M. Owczarz, S. Bolisetty, R. Mezzenga, P. Arosio, *J. Colloid Interface Sci.* **2015**, *437*, 244 – 251.
[6] Y. Hou, M. Brower, D. Pollard, D. Kanani, R. Jacquemart, B. Kachuik, J. Stout, *Biotechnol. Prog.* **2015**, *31*, 974 – 982.
[7] R. L. Rill, D. H. Van Winkle, B. R. Locke, *Anal. Chem.* **1998**, *70*, 2433 – 2438.
[8] B. Amsden, *Macromolecules* **1998**, *31*, 8382 – 8395.
[9] J. Kärger, *ChemPhysChem* **2015**, *16*, 24 – 51.
[10] J. Siepmann, N. A. Peppas, *Adv. Drug Delivery Rev.*. **2001**, *48*, 139 – 157.
[11] V. Hagel, T. Haraszti, H. Boehm, *Biointerphases* **2013**, *8*, 36.
[12] R. K. Lewus, G. Carta, *Ind. Eng. Chem. Res.* **2001**, *40*, 1548 – 1558.
[13] J. Siepmann, K. Siepmann, *Int. J. Pharm.* **2008**, *364*, 328 – 343.
[14] G. S. Crank, *Diffusion in Polymers*, Academic, New York, **1968**.
[15] N. A. Peppas, C. T. Reinhart, *J. Membr. Sci.* **1983**, *15*, 275 – 287.
[16] D. Caccavo, S. Cascone, G. Lamberti, A. A. Barba, *Mol. Pharm.* **2015**, *12*, 474 – 483.
[17] L. Masaro, X. X. Zhu, *Prog. Polym. Sci.* **1999**, *24*, 731 – 775.
[18] I. Kohli, A. Mukhopadhyay, *Macromolecules* **2012**, *45*, 6143 – 6149.
[19] M. Ferro, F. Castiglione, C. Punta, L. Melone, W. Panzeri, B. Rossi, F. Trotta, A. Mele, *Beilstein J. Org. Chem.* **2014**, *10*, 2715 – 2723.
[20] Y. Fu, W. J. Kao, *Expert Opin. Drug Delivery* **2010**, *7*, 429 – 444.
[21] M. Santoro, P. Marchetti, F. Rossi, G. Perale, F. Castiglione, A. Mele, M. Masi, *J. Phys. Chem. B* **2011**, *115*, 2503 – 2510.
[22] T. Casalini, M. Salvalaglio, G. Perale, M. Masi, C. Cavallotti, *J. Phys. Chem. B* **2011**, *115*, 12896 – 12904.
[23] G. Perale, P. Arosio, D. Moscatelli, V. Barri, M. Muller, S. Maccagnan, M. Masi, *J. Controlled Release* **2009**, *136*, 196 – 205.
[24] Y. T. Kim, J. M. Caldwell, R. V. Bellamkonda, *Biomaterials* **2009**, *30*, 2582 – 2590.
[25] D. W. Brann, K. Dhandapani, C. Wakade, V. B. Mahesh, M. M. Khan, *Steroids* **2007**, *72*, 381 – 405.
[26] T. Azaïs, C. Tourné-Péteilh, F. Aussenac, N. Baccile, C. Coelho, J. M. Devoisselle, F. Babonneau, *Chem. Mater.* **2006**, *18*, 6382 – 6390.
[27] M. L. Vueba, M. E. Pina, L. A. E. B. De Carvalho, *J. Pharm. Sci.* **2008**, *97*, 845 – 859.
[28] J. E. Jenkins, M. R. Hibbs, T. M. Alam, *ACS Macro Lett.* **2012**, *1*, 910 – 914.
[29] T. M. Alam, M. R. Hibbs, *Macromolecules* **2014**, *47*, 1073 – 1084.
[30] G. Perale, F. Rossi, M. Santoro, P. Marchetti, A. Mele, F. Castiglione, E. Raffa, M. Masi, *J. Biomed. Nanotechnol.* **2011**, *7*, 476 – 481.
[31] E. B. Schirmer, G. Carta, *Aiche J.* **2009**, *55*, 331 – 341.
[32] F. Rossi, F. Castiglione, M. Ferro, P. Marchini, E. Mauri, M. Moioli, A. Mele, M. Masi, *ChemPhysChem* **2015**, *16*, 2818 – 2825.
[33] S. Lerdkanchanaporn, D. Dollimore, *J. Therm. Anal. Calorim.* **1997**, *49*, 879 – 886.
[34] W. Ali, A. C. Williams, C. F. Rawlinson, *Int. J. Pharm.* **2010**, *391*, 162 – 168.
[35] I. Caron, F. Rossi, S. Papa, R. Aloe, M. Sculco, E. Mauri, A. Sacchetti, E. Erba, N. Panini, V. Parazzi, M. Barilani, G. Forloni, G. Perale, L. Lazzari, P. Veglianese, *Biomaterials* **2016**, *75*, 135 – 147.
[36] F. Rossi, G. Perale, G. Storti, M. Masi, *J. Appl. Polym. Sci.* **2012**, *123*, 2211 – 2221.
[37] P. J. Flory, *Principles of polymer chemistry*, Cornell Univeristy Press, New York, **1953**.
[38] S. J. de Jong, B. van Eerdenbrugh, C. F. van Nostrum, J. J. Kettenes-van de Bosch, W. E. Hennink, *J. Controlled Release* **2001**, *71*, 261 – 275.
[39] I. Lopez Arbeloa, *J. Chem. Soc. Faraday Trans.* **1981**, *77*, 1735 – 1742.
[40] P. L. Ritger, N. A. Peppas, *J. Controlled Release* **1987**, *5*, 23 – 36.

Manuscript received: January 18, 2016
Accepted Article published: February 25, 2016
Final Article published: March 21, 2016